Sustained greening of the Antarctic Peninsula observed from satellites

Thomas P. Roland [1,6] ✉, Oliver T. Bartlett [1,2,6] ✉, Dan J. Charman [1], Karen Anderson [3], Dominic A. Hodgson [4], Matthew J. Amesbury [5], Ilya Maclean [3], Peter T. Fretwell [4] & Andrew Fleming [4]

The Antarctic Peninsula has experienced considerable anthropogenic warming in recent decades. While cryospheric responses are well defined, the responses of moss-dominated terrestrial ecosystems have not been quantified. Analysis of Landsat archives (1986–2021) using a Google Earth Engine cloud-processing workflow suggest widespread greening across the Antarctic Peninsula. The area of likely vegetation cover increased from 0.863 km^2 in 1986 to 11.947 km^2 in 2021, with an accelerated rate of change in recent years (2016–2021: 0.424 km^2 yr^{-1}) relative to the study period (1986–2021: 0.317 km^2 yr^{-1}). This trend echoes a wider pattern of greening in cold-climate ecosystems in response to recent warming, suggesting future widespread changes in the Antarctic Peninsula's terrestrial ecosystems and their long-term functioning.

Antarctica has experienced significant increases in temperature over the past 60 years[1], with rates of warming highest in the West Antarctic and Antarctic Peninsula (AP) regions[2] and occurring much faster than global average warming[3]. Despite a recent pause in warming (1999–2014) across the AP, linked to short-term natural climate variability[3], the prevailing direction and magnitude of warming across the AP is clear[4], and the trend is expected to continue at 0.34 °C per decade until 2100[5]. Climate model projections suggest that regional temperature rise will remain well above the global average, be greater in austral winter than in summer and be associated with higher precipitation and increases in the growing season[6].

With over 90% of the AP's glaciers losing mass since the 1940s[7], assessments of the impacts of and feedbacks from Antarctic climate change in the AP region have focused largely on cryospheric response, especially the more temperature-sensitive glaciers at the fringes of the continent[8]. Although changes in the cryosphere are critical to global sea-level change, a potential threefold increase in ice-free area on the AP by the end of the century also means it is critical to understand terrestrial biological shifts for this region, which already holds the majority of Antarctica's terrestrial vegetation[9].

Addressing questions about AP vegetation extent and change is important as amelioration of AP climate, together with associated recession in ice and snow cover, could increase connectivity between the AP's distinct Antarctic Conservation Biogeographic Regions[10,11], resulting in regional-scale ecological homogenization, reorganization of species and communities, increased productivity and soil development, and changes in trophic interactions[9,12].

Furthermore, species translocation over distances far greater than natural dispersal ranges[13] and the introduction of non-native, potentially invasive species[14] could further erode biodiversity and threaten endemic species. With a flow of new seed sources to the continent associated with tourism and scientific research footfall, biosecurity will become increasingly critical as temperature limitations on cold, high-latitude ecosystems decrease[15], removing constraints on colonization by non-native species.

Vascular plants native to the AP have already been shown to have experienced recent extensions to their range[16,17], but it is the region's moss ecosystems (Fig. 1) that are pivotal in terms of changes in the spatial extent of vegetated ground cover[18], organic soil formation[19] and higher plant colonization[20]. The vertical accumulation of moss bank systems (Fig. 1c) has tracked the long-term trend in multi-decadal warming in the region[21–23], but major questions remain over the existence, continuity and controls on lateral spread of moss-dominated systems.

[1]Geography, Faculty of Environment, Science and Economy, University of Exeter, Devon, UK. [2]Geography, Environment and Planning, School of Life and Medical Sciences, University of Hertfordshire, Hatfield, UK. [3]Environment and Sustainability Institute, Faculty of Environment, Science and Economy, University of Exeter, Penryn, UK. [4]British Antarctic Survey, Cambridge, UK. [5]Research Services, University of Exeter, Devon, UK. [6]These authors contributed equally: Thomas P. Roland, Oliver T. Bartlett. ✉e-mail: t.p.roland@exeter.ac.uk; o.bartlett@herts.ac.uk

Fig. 1 | Moss-dominated ecosystems across the AP. a, Moss hummocks, Ardley Island (62° S). **b**, Moss lawn, or carpet, Barrientos Island (62° S). **c**, Moss bank on bare rock, Norsel Point (64° S).

Moss communities have a central role in the conversion of bare rock surfaces to vegetated ground (for example, Fig. 1), so understanding the rate, nature and controls on changes in moss-dominated ecosystems is critical to addressing the question of whether an Antarctic 'greening'—in line with global trends[24] and comparable to ongoing but complex trends observed in the Arctic[25]—is now under way and will presage a radical future shift in the terrestrial biology of this iconic region.

This study aimed to assess vegetation response to climate change on the AP over the past 35 years by quantifying rates of change in the spatial extent and 'direction' (greening versus browning[25]), which have not yet been quantified. In this Article, we apply the cloud-processing capabilities of the Google Earth Engine platform, using data from the Landsat archive[26] to examine trends in vegetation indices, including Normalized Difference Vegetation Index (NDVI) and Tasseled Cap Greenness (TCG)[27,28], from 1986 to 2021. NDVI is a well-established metric for monitoring vegetation using multispectral imagery. It is based on the ratio between the reflectance of visible red and that of near-infrared light. Based on previous work undertaken on the AP, an NDVI threshold of >0.2 is taken to indicate the 'almost certain' presence

of vegetation[29]. TCG, originally developed for use in agricultural contexts, offers an alternative metric to NDVI, whereby a transformation is applied to multiple spectral bands to emphasize the vegetation signal. TCG therefore has the potential to be more sensitive to the transition between bare soil and emerging vegetation[27]. Because of the AP's limited botanical diversity and the relative absence of higher plants, a greening trend in these indices would be interpreted as indicating primarily increased vegetation abundance and cover by the region's various moss-dominated ecosystems (Fig. 1).

## Results and discussion

A greener AP

Previous evidence for terrestrial biological change on the AP was based on historical observations of plant cover at individual sites from the 1960s onwards[17,30], together with longer-term decadal-to-centennial resolution palaeoecological records, which have demonstrated increases in moss bank productivity and vertical accumulation from across the AP since ~1950 that are significant in the context of the late Holocene[21,22,31]. Rates of lateral expansion of moss-dominated ecosystems have the potential to be several orders of magnitude higher than vertical growth rates[32,33]. Satellite-derived measurements of vegetation extent and distribution allow for broader quantification of change than in situ observations, but for the AP such data currently exist only for a single year (2001)[29]. This study presents annual–decadal trends and rates of change for the entire Peninsula over the past 35 years (Figs. 2 and 3).

In this article, we demonstrate a clear but nonlinear trend towards a greater area of vegetation cover (NDVI > 0.2; Fig. 2) across the AP in recent decades, increasing from 0.863 km^2 (1986) to 11.947 km^2 (2021). This increase is statistically significant (Mann–Kendall τ = 2.31, P = 0.021; Supplementary Table 5.2) and confirms that short-term changes in vegetation cover are identifiable and measurable in this context. Crucially, the rate of change in vegetation cover has increased considerably in recent years (2016–2021: 0.424 km^2 yr^{-1}) relative to the full study period (1986–2021: 0.317 km^2 yr^{-1}) and previous windows of analysis (1986–2004: 0.291 km^2 yr^{-1}; 2004–2016: 0.310 km^2 yr^{-1}) (Supplementary Table 5.1; note that sensor transitions and radiometric differences were accounted for[34]). Results indicate significant positive increases in vegetation cover that are widespread across the western AP, extending from ~68.5° S—close to the global southern limit of flowering plants and moss-dominated ecosystems[35]—to the northern limit of South Shetland archipelago at ~61° S (Fig. 3). All temporal trends (Supplementary Tables 5.1 and 5.2) and spatial patterns (Supplementary Fig. 4.2) of positive change in vegetation cover through the study period recorded using NDVI are echoed in TCG results and are, again, statistically significant (TCG > 0 area 1986–2021; Mann–Kendall τ = 2.54, P = 0.011).

It is possible that a lengthening of the growing season on the AP could be contributing, increasingly through to the later years of the window of analysis, to some of the apparent increase in the number of pixels classified as vegetation by the threshold of detection (NDVI > 0.2). However, extensive field validation over a number of years would be required to confirm the proportion of the overall greening trend that could be attributed to this effect.

Persistent cloud cover across the AP[36] presents a considerable challenge to routine monitoring of the land surface in the region using remote sensing. We quantified the relationship between interannual variation in ice-free observable land area and vegetated area (Fig. 2), finding only weak positive correlations with either vegetation index (NDVI R^2 = 0.351; TCG R^2 = 0.272; Supplementary Fig. 3.2). This supports the assertion that the positive trends in vegetation cover (NDVI and TCG) are not simply artefacts of observable land area or greater data availability in recent years, but rather are reflective of an expansion of plant life driving a widespread recent greening of the AP.

In addition, analysis of very-high-resolution, cloud-free WorldView-2 (2 m grain) imagery for the area surrounding Robert
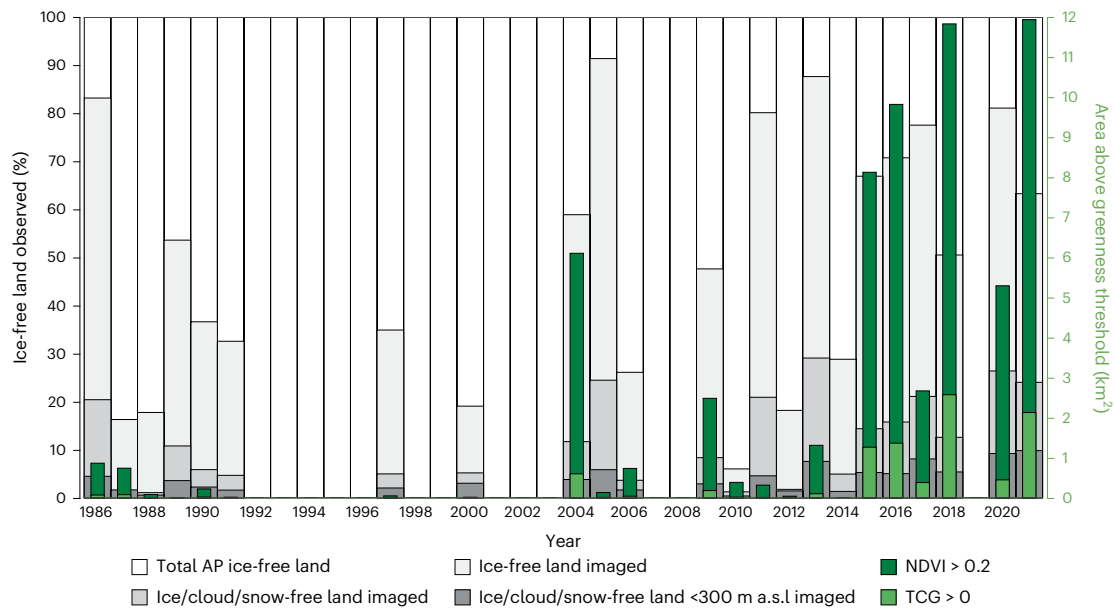
Fig. 2 | Change in the areal extent of likely vegetation cover. Based on NDVI (>0.2 threshold, dark green bars) and TCG (>0 threshold, light green bars) vegetation indices across the AP derived from Landsat 5–8 data (1986–2021). Grey shaded bars indicate the percentage of ice-, cloud- and snow-free land observable during March of each year, plotted against total ice-free land on the AP (as measured during austral summer, 2013–2015, using Landsat 8 imagery). A mask was added to eliminate land above 300 m above sea level (a.s.l.) to reduce reflectance issues from high-latitude and high-altitude areas, which may erroneously indicate the presence of moss in areas beyond known limits of growth. See Supplementary Fig. 4.1 for TCG time series in isolation.
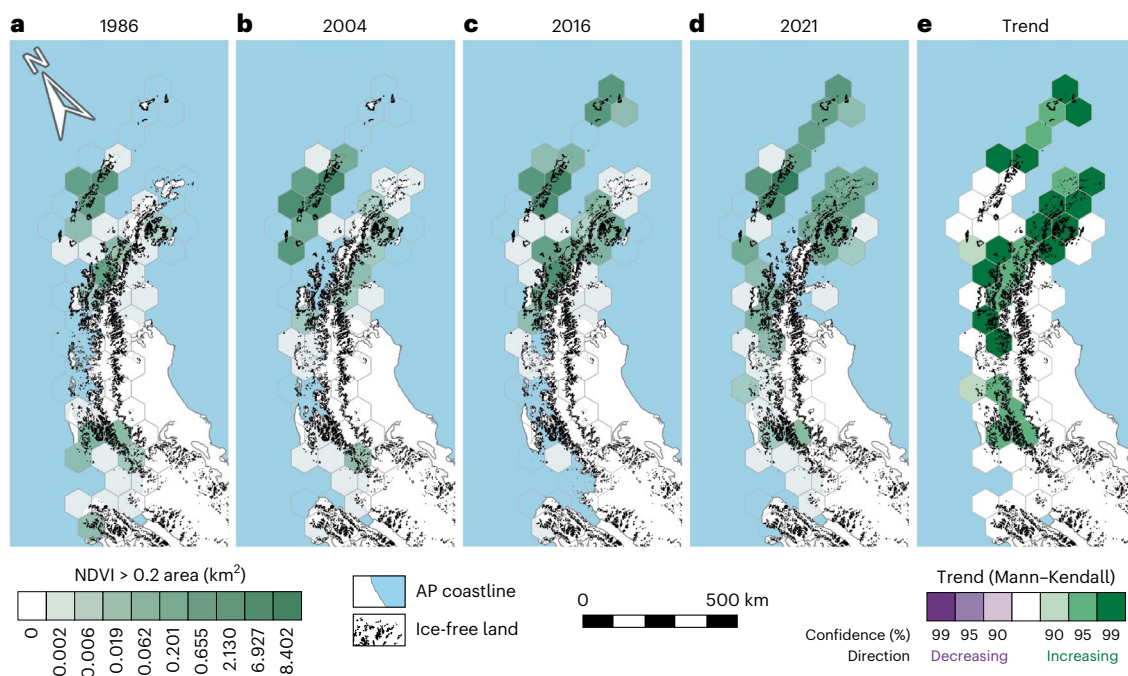
Fig. 3 | Spatial and temporal complexity in AP greening trend over the past 35 years. a–d, Vegetated area (km², <300 m a.s.l.) in the years 1986 (**a**), 2004 (**b**), 2016 (**c**) and 2021 (**d**) based on Landsat 5–8 data. The hexagons each represent 5,000 km² and are coloured according to the area of NDVI > 0.2 they contain, therefore allowing for systematic visualization of greening trends despite the relatively small proportion of ice-free land compared with ice-covered land and ocean. The presented years were chosen on the basis of percentage of land imaged, highest area with NDVI > 0.2 and temporal spacing through the time series (see Fig. 2 for detail). **e**, Mann–Kendall trend analysis results for all available years (1985–2021) showing direction of trend and confidence level. See Supplementary Fig. 4.2 for the TCG equivalent of this figure. Coastline and ice-free land are shown by the black outline[49].

Island—an area known to be vegetated and considered broadly characteristic of the northern AP, where the greening trend is greatest (Fig. 3)—shows an 18.7% increase in vegetated area between 2013 and 2016 (Supplementary Section 3.3). This localized analysis highlights that the rates observed through the Landsat archive, across its multiple sensors and across the AP are coherent with those measured at higher resolution by a single sensor.

This recent acceleration in the rate of change in vegetation cover (2016–2021) coincides with a marked decrease in sea-ice extent in Antarctica over the same period[37]. A subsequent increase in open water,

coupled with a strongly positive Southern Annular Mode[38], could be resulting in warmer, wetter conditions[39] favourable for plant growth as a result of higher moisture availability.

Short-term variability in greening

In addition to the interannual variation in satellite observation conditions, the nonlinearity seen in our time series (Fig. 2) is probably driven by temporal complexity in greening and browning trends, comparable to that seen in the Arctic[25]. This is echoed spatially (Fig. 3), highlighting mechanistic uncertainty around local-scale meteorological variability and plant response as the AP shifts towards warmer and wetter conditions[6]. Some change might be expected given global shifts in greenness[24], but the complexity of Arctic greening and browning of moss-dominated ecosystems in satellite-derived vegetation indices[25] and variability in Antarctic moss health related to moisture availability[40] are potential hypotheses explaining the absence of a simple linear shift towards a greener AP. For example, across the southern section of King George and Ardley islands, we demonstrate the spatial complexity of localized greening and browning trends (Fig. 4), which occur concurrently with overall and increasing regional trends in the lateral expansion of moss ecosystems (Figs. 2 and 3).

Analysis of very-high-resolution imagery of the Robert Island region revealed that areas of well-established vegetation exhibited only minor changes in greenness, with the largest of such areas demonstrating a slight browning trend (Supplementary Section 3.3). The overall increase in vegetation cover through the analysed period (2013–2016) here has instead been driven largely by rapidly increasing vegetation cover in what appear to be newly colonized areas, providing mechanistic support for the rates of lateral expansion of vegetation measured in the Landsat archive.

While future large-scale vegetation change on the AP will ultimately be driven by macroclimate, the behaviour of the poikilohydric mosses that dominate these ecosystems is likely to be strongly modified by localized microclimatic topographical controls[23]. This is potentially evidenced by the browning trend (2016–2021) seen on the eastern side of Ardley Island (Fig. 4), leeward of the dominant southern westerly wind regime, with local topography modulating moisture availability through its effect on orographic precipitation and desiccating wind, in addition to localized climate variability[40]. These observations are based solely on the comparison of conditions in 2021 with areas that were also observable in 2016 and are therefore not artefacts of data availability owing to cloud cover (Supplementary Fig. 2.3 and Supplementary Section 3.2). Such patterns are likely to be further confounded by an increasing potential for interannual climatic variability, potentially exacerbated by extreme temperature events (for example, record-breaking heatwaves of the 2019–2020 austral summer[41]), and it is clear that further understanding is needed of the effects of both prevailing and extreme climatic change on ecohydrology in the AP's moss-dominated ecosystems. A further factor that must be considered when interpreting localized greening/browning trends is the presence of penguin colonies and their potential to cause or exacerbate localized trends in both greening (in the longer term due to N enrichment[42]) and browning (in the shorter term due to trampling and guano build-up). For example, portions of the area of browning seen on the eastern side of Ardley Island (Fig. 4) overlap with the current penguin nesting area[43], further highlighting the need for ground-based validation to resolve these complexities.

Given the spatial and temporal complexity demonstrated here (Figs. 2 and 3), any future assessment of vegetation response to climate change on the AP must be supplemented by ground-based data collection and consider all trajectories towards greening, including the (1) increased productivity and vigour of existing vegetation[44,45], (2) spatial expansion of existing vegetation communities and (3) creation of new vegetation communities through species migration.
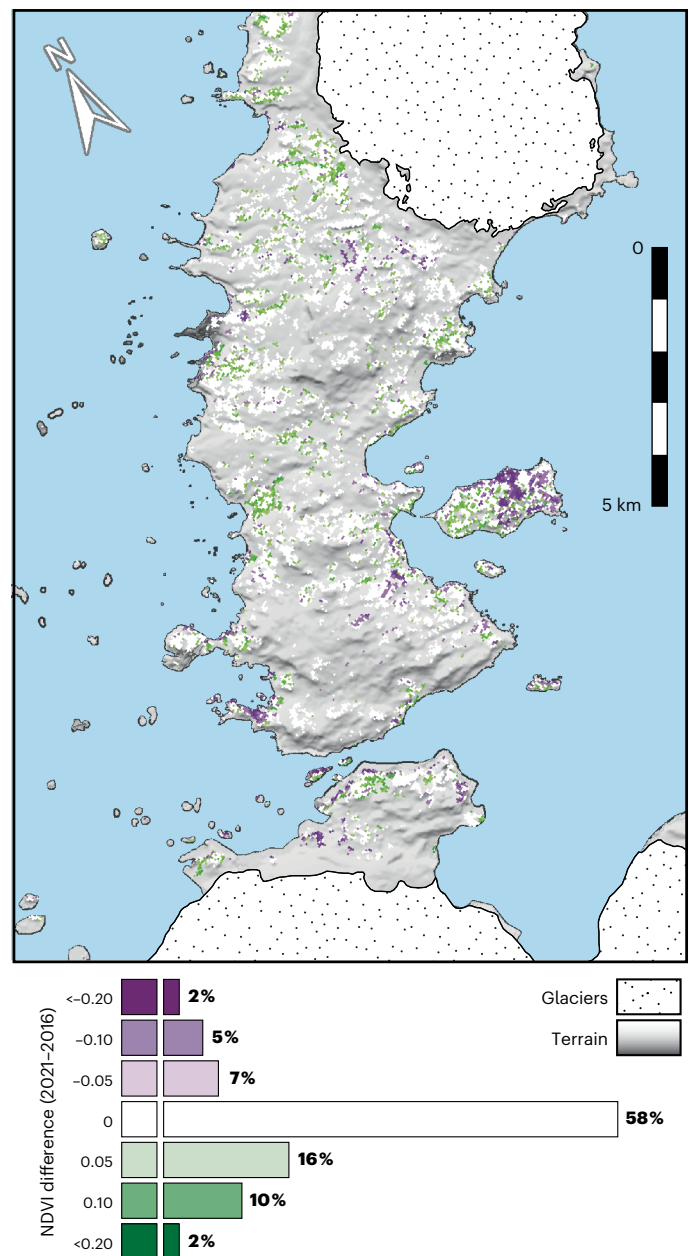
Fig. 4 | Spatial complexity in the recent localized greening (and browning) trend for the southern section of King George Island and Ardley Island. Trend demonstrated by comparing differences (2021–2016) in NDVI for areas vegetated (NDVI > 0.2) in 2016. Classes follow 'confidence' intervals for vegetated areas on the AP[29] (NDVI > 0.05, probable likelihood; NDVI > 0.1, very probable; NDVI > 0.2, almost certain). Coastline and ice-free land are shown by the black outline[49].

Greening and the future

Regardless of the complexities discussed in the preceding, the overall statistically significant trajectory of AP-wide greening (Fig. 2) from 1986 to 2021, exemplified in the temporal snapshots presented in Fig. 3, provides strong evidence of rapid and ongoing response of AP vegetation to climate change, and presents a compelling case for future widespread changes in the AP's terrestrial ecosystems. The exploration of AP greening trends through recent decades presented here represents a systematically rigorous approach (Methods and Supplementary Information). The spatial patterns of greening observed are consistent with our understanding of the modern distribution of moss-dominated ecosystems across the AP[29], suggesting that these trends are being driven by increased productivity, vigour and lateral

expansion of existing vegetation. This echoes observations made of similar ecosystems across the high Arctic[25] and in mountainous areas[46,47] under climate change and reflects wider global patterns of greening in cold-climate ecosystems in response to recent warming[15]. Global modelling work—not yet extended to the AP—identifies a widespread decline over recent decades in the area of land where vegetation is limited by temperature. This is expected to continue under future warming scenarios and result in widespread greening in cold regions[15]. If this anticipated trend extends to the AP, as our findings suggest is likely, it would have implications for the long-term functioning of the peninsula's terrestrial ecosystems.

Furthermore, mosses are capable of colonizing bare rock surfaces and provide the basis for future soil development as a substrate for the consolidation of moss-dominated ecosystems, as well as colonization by higher plants[12,19,20]. If recent warming has driven an increase in biological productivity[22,31], it is predicted that soil development will have followed similar patterns to those seen in Figs. 3 and 4, be mostly recent in origin and located in areas that have more favourable microclimatic conditions (warmer and wetter), potentially enhanced by N enrichment from guano[42].

Native vascular plants are already demonstrating range expansions across the AP[16,17], but questions remain over the role that lateral expansion of moss ecosystems, longer-distance and bare-rock colonization by mosses and any associated soil formation, may play in providing a vector for further ecological translocation of vascular plants, including non-native, potentially invasive species—the threat of which is increasingly recognized[13,14,48].

Ultimately, a clear understanding of the nature and future of biological responses across the AP to Antarctic climate change is limited by a relative lack of long-term data. The work presented here provides a remote-sensing baseline against which to track the extent and nature of Antarctic greening—a trend that these results imply is now under way. We anticipate that future work can be informed by further ground-based validation and projection modelling of both (micro) climate and species distribution. Combined, this work has the potential to inform effective and essential biosecurity governance of the AP and wider Antarctic region in the longer term.

Online content

Any methods, additional references, Nature Portfolio reporting summaries, source data, extended data, supplementary information, acknowledgements, peer review information; details of author contributions and competing interests; and statements of data and code availability are available at https://doi.org/10.1038/s41561-024-01564-5.

References

1. Turner, J. et al. Antarctic climate change during the last 50 years. *Int. J. Climatol.* **25**, 279–294 (2005).
2. Nicolas, J. P. & Bromwich, D. H. New reconstruction of Antarctic near-surface temperatures: multidecadal trends and reliability of global reanalyses. *J. Clim.* **27**, 8070–8093 (2014).
3. Turner, J. et al. Absence of 21st century warming on Antarctic Peninsula consistent with natural variability. *Nature* **535**, 411–415 (2016).
4. Turner, J. et al. Antarctic temperature variability and change from station data. *Int. J. Climatol.* **40**, 2986–3007 (2020).
5. IPCC *Climate Change 2014: Synthesis Report* (eds Core Writing Team et al.) (IPCC, 2014).
6. Siegert, M. et al. The Antarctic Peninsula under a 1.5 °C global warming scenario. *Front. Environ. Sci.* **7**, 102 (2019).
7. Cook, A. J., Vaughan, D. G., Luckman, A. J. & Murray, T. A new Antarctic Peninsula glacier basin inventory and observed area changes since the 1940s. *Antarct. Sci.* **26**, 614–624 (2014).
8. Cook, A. J. et al. Ocean forcing of glacier retreat in the western Antarctic Peninsula. *Science* **353**, 283–286 (2016).
9. Lee, J. R. et al. Climate change drives expansion of Antarctic ice-free habitat. *Nature* **547**, 49–54 (2017).
10. Terauds, A. et al. Conservation biogeography of the Antarctic. *Divers. Distrib.* **18**, 726–741 (2012).
11. Terauds, A. & Lee, J. R. Antarctic biogeography revisited: updating the Antarctic Conservation Biogeographic Regions. *Divers. Distrib.* **22**, 836–840 (2016).
12. Convey, P. & Peck, L. S. Antarctic environmental change and biological responses. *Sci. Adv.* **5**, eaaz0888 (2019).
13. Hughes, K. A. et al. Human-mediated dispersal of terrestrial species between Antarctic biogeographic regions: a preliminary risk assessment. *J. Environ. Manag.* **232**, 73–89 (2019).
14. Hughes, K. A. et al. Invasive non-native species likely to threaten biodiversity and ecosystems in the Antarctic Peninsula region. *Glob. Change Biol.* **26**, 2702–2716 (2020).
15. Keenan, T. F. & Riley, W. J. Greening of the land surface in the world's cold regions consistent with recent warming. *Nat. Clim. Change* **8**, 825–828 (2018).
16. Hill, P. W. et al. Vascular plant success in a warming Antarctic may be due to efficient nitrogen acquisition. *Nat. Clim. Change* **1**, 50–53 (2011).
17. Parnikoza, I. et al. Current status of the Antarctic herb tundra formation in the Central Argentine Islands. *Glob. Change Biol.* **15**, 1685–1693 (2009).
18. Convey, P. et al. The spatial structure of Antarctic biodiversity. *Ecol. Monogr.* **84**, 203–244 (2014).
19. Ugolini, F. C. & Bockheim, J. G. Antarctic soils and soil formation in a changing environment: a review. *Geoderma* **144**, 1–8 (2008).
20. Casanova-Katny, M. A. & Cavieres, L. A. Antarctic moss carpets facilitate growth of *Deschampsia antarctica* but not its survival. *Polar Biol.* **35**, 1869–1878 (2012).
21. Royles, J. et al. Plants and soil microbes respond to recent warming on the Antarctic Peninsula. *Curr. Biol.* **23**, 1702–1706 (2013).
22. Amesbury, M. J. et al. Widespread biological response to rapid warming on the Antarctic Peninsula. *Curr. Biol.* **27**, 1616–1622 (2017).
23. Royles, J. et al. Moss stable isotopes (carbon-13, oxygen-18) and testate amoebae reflect environmental inputs and microclimate along a latitudinal gradient on the Antarctic Peninsula. *Oecologia* **181**, 931–945 (2016).
24. Zhu, Z. et al. Greening of the Earth and its drivers. *Nat. Clim. Change* **6**, 791–795 (2016).
25. Myers-Smith, I. H. et al. Complexity revealed in the greening of the Arctic. *Nat. Clim. Change* **10**, 106–117 (2020).
26. Gorelick, N. et al. Google Earth Engine: planetary-scale geospatial analysis for everyone. *Remote Sens. Environ.* **202**, 18–27 (2017).
27. Kauth, R. J. & Thomas, G. S. The tasselled cap—a graphic description of the spectral–temporal development of agricultural crops as seen by LANDSAT. *LARS Symp.* **159**, 41–51 (1976).
28. Baig, M. H. A., Zhang, L., Shuai, T. & Tong, Q. Derivation of a tasselled cap transformation based on Landsat 8 at-satellite reflectance. *Remote Sens. Lett.* **5**, 423–431 (2014).
29. Fretwell, P. T., Convey, P., Fleming, A. H., Peat, H. J. & Hughes, K. A. Detecting and mapping vegetation distribution on the Antarctic Peninsula from remote sensing data. *Polar Biol.* **34**, 273–281 (2011).
30. Fowbert, J. A. & Lewis Smith, R. I. Rapid population increases in native vascular plants in the Argentine Islands, Antarctic Peninsula. *Arct. Alp. Res.* **26**, 290–296 (1994).
31. Charman, D. J. et al. Spatially coherent late Holocene Antarctic Peninsula surface air temperature variability. *Geology* **46**, 1071–1074 (2018).
32. Granlund, L. et al. Recent lateral expansion of *Sphagnum* bogs over central fen areas of boreal aapa mire complexes. *Ecosystems* **25**, 1455–1475 (2022).

33. Juselius-Rajamäki, T., Väliranta, M. & Korhola, A. The ongoing lateral expansion of peatlands in Finland. *Glob. Change Biol.* **29**, 7173–7191 (2023).

34. Roy, D. P. et al. Characterization of Landsat-7 to Landsat-8 reflective wavelength and Normalized Difference Vegetation Index continuity. *Remote Sens. Environ.* **185**, 57–70 (2016).

35. Convey, P., Hopkins, D. W., Roberts, S. J. & Tyler, A. N. Global southern limit of flowering plants and moss peat accumulation. *Polar Res.* **30**, 8929 (2011).

36. Lachlan-Cope, T. Antarctic clouds. *Polar Res.* **29**, 150–158 (2010).

37. Fetterer, F., Knowles, K., Meier, W. M., Savoie, M. & Windnagel, A. K. Sea Ice Index v.3. *NSIDC* https://doi.org/10.7265/N5K072F8 (2017).

38. Wachter, P., Beck, C., Philipp, A., Höppner, K. & Jacobeit, J. Spatiotemporal variability of the Southern Annular Mode and its influence on Antarctic surface temperatures. *J. Geophys. Res. Atmos.* **125**, e2020JD033818 (2020).

39. Clem, K. R. & Fogt, R. L. Varying roles of ENSO and SAM on the Antarctic Peninsula climate in austral spring. *J. Geophys. Res. Atmos.* **118**, 11481–11492 (2013).

40. Robinson, S. A. et al. Rapid change in East Antarctic terrestrial vegetation in response to regional drying. *Nat. Clim. Change* **8**, 879–884 (2018).

41. Robinson, S. A. et al. The 2019/2020 summer of Antarctic heatwaves. *Glob. Change Biol.* **26**, 3178–3180 (2020).

42. Wasley, J. et al. Bryophyte species composition over moisture gradients in the Windmill Islands, East Antarctica: development of a baseline for monitoring climate change impacts. *Biodiversity* **13**, 257–264 (2012).

43. Roberts, S. J. et al. Past penguin colony responses to explosive volcanism on the Antarctic Peninsula. *Nat. Commun.* **8**, 14914 (2017).

44. Malenovský, Z., Lucieer, A., King, D. H., Turnbull, J. D. & Robinson, S. A. Unmanned aircraft system advances health mapping of fragile polar vegetation. *Methods Ecol. Evol.* **8**, 1842–1857 (2017).

45. Turner, D., Lucieer, A., Malenovský, Z., King, D. & Robinson, S. A. Assessment of Antarctic moss health from multi-sensor UAS imagery with random forest modelling. *Int. J. Appl. Earth Obs. Geoinf.* **68**, 168–179 (2018).

46. Rumpf, S. B. et al. From white to green: snow cover loss and increased vegetation productivity in the European Alps. *Science* **376**, 1119–1122 (2022).

47. Kellner, J. R., Kendrick, J. & Sax, D. F. High-velocity upward shifts in vegetation are ubiquitous in mountains of western North America. *PLoS Clim.* **2**, e0000071 (2023).

48. Chwedorzewska, K. J., Korczak-Abshire, M. & Znój, A. Is Antarctica under threat of alien species invasion? *Glob. Change Biol.* **26**, 1942–1943 (2020).

49. Burton-Johnson, A., Black, M., Peter, T. F. & Kaluza-Gilbert, J. An automated methodology for differentiating rock from snow, clouds and sea in Antarctica from Landsat 8 imagery: a new rock outcrop map and area estimation for the entire Antarctic continent. *Cryosphere* **10**, 1665–1677 (2016).

Methods

Data

Systematic exploration of the NASA (National Aeronautics and Space Administration) Landsat satellite mission archives using Google Earth Engine provided the longest time series of suitable imagery possible (1986–2021) from across the AP, at medium resolution (30 m² grain). Tier 2, top-of-atmosphere reflectance imagery was used because this was the only available imagery at the time of the study. For reliable comparison across years, the imagery dataset was filtered by month, cloud cover over land percentage and image quality.

First, for consistency across the entire study time series and to maximize vegetated pixel returns, the dataset was filtered to include only images captured in March. Previous remote sensing of vegetation in the AP has been conducted using either February imagery[29] or composites of February and March imagery[50]. Ecologically, March is most likely to be the end of the growing season, where temperatures across the region have been highest annually for the previous three months in the austral summer[22]. Preliminary analysis of January, February and March imagery showed vegetated pixel returns were typically highest in March (Supplementary Table 1.1). Furthermore, the maximum measured vegetated area was observed in March (7.64 km²; Supplementary Table 1.1).

Second, the Landsat dataset was filtered to source imagery where cloud cover over land was less than 40%. As image cloud cover percentage in the AP is regularly 80–90%[35], image availability is restricted. However, preliminary analysis found the 40% filter maximized the number of images ingested into the workflow along with computational efficiency. For example, increasing the cloud cover filter to 50% resulted in a 3× increase in processing time and negligible difference in detected vegetation.

Finally, Landsat images are assigned a quality value from worst (0) to best (9) in preprocessing by the United States Geological Survey[51]. Due to the difficulties with geometric correction of earlier imagery, the use of top-of-atmosphere reflectance imagery and to ensure consistency across satellites, only images assigned a quality value of 9 were used. In addition, Landsat 4, 5 and 7 imagery was radiometrically calibrated to Landsat 8 imagery using the previously published coefficients[34]. Previous studies have employed this calibration in the Himalayas, where vegetation is similarly low stature and sparsely distributed[52]. However, the calibration[34] is not a correction. Hence the differences in distribution of greenness index returns were compared between overlapping Landsat 7 Enhanced Thematic Mapper Plus (ETM+) and Landsat 8 Operational Land Imager (OLI) scenes to quantify further required adjustments (detailed in Supplementary Section 1.2).

After calibration, Landsat ETM+ data were found to underestimate NDVI > 0.2 areas by approximately 10% (9.58%; Supplementary Table 1.2). Similarly, TCG areas were underestimated in ETM imagery compared with Landsat 8 OLI imagery (5.68%; Supplementary Table 1.3). As Landsat 4 and 5's Thematic Mapper and Landsat 7 ETM+ have been shown to be sufficiently radiometrically similar, the transformation coefficients used to calibrate to OLI were the same[34]. Hence NDVI-estimated area values from Landsat 4, 5 and 7 were increased by 10% and TCG areas by 6%.

Greenness indices

NDVI and TCG were determined for each Landsat image. NDVI, based on the ratio of reflectance of visible red to near-infrared light, has been shown to provide meaningful measurements of green biomass even in landscapes characterized by sparse vegetation of low stature[52]. Ground-truthing of NDVI values from Landsat data from the AP suggests several possible thresholds at which to classify vegetation as present (NDVI > 0.05, probable likelihood; NDVI > 0.1, very probably; NDVI > 0.2, almost certain)[29]. A threshold of 0.2 was selected despite the relative sparsity of vegetation so that confidence in returns would be maximized in the absence of field validation. This approach represents the almost certain level of confidence in vegetation presence[29]. TCG was implemented as a first-order validation of any trends observed in the NDVI signal as it is less sensitive to bidirectional reflectance distribution function effects. TCG can more reliably distinguish background brightness effects than NDVI, hence the signal is more responsive to the presence of low-stature and non-leafy vegetation on bright soils or bare rock surfaces[53] such as those found on the AP (Fig. 1) (for example expansion at the fringes of established moss carpets and new areas of colonization). In addition, moss-dominated systems exhibit a robust TCG signal only if they are well established[54]. Hence it was expected that TCG area values would be markedly less than NDVI, but where the trend was concomitant, it would support the NDVI results. Coefficients used to derive TCG are outlined in the code (Supplementary Section 6). To determine the maximum lateral extent of vegetation in the region for a given year, annual mosaics of maximum NDVI and TCG were generated.

NDVI has been used to monitor mosses effectively in maritime regions of Antarctica, including in our study region[55], and is therefore well suited to our aims of mapping the occurrence of moss-dominated vegetation in individual years. Conversely, the TCG response shows positive values in well-vegetated areas but negative values in areas with more mixed pixels (Supplementary Fig. 3.4), suggesting that in mixed pixels there are alterations to surface reflectance that maintain an NDVI > 0.2 but lessen the response of TCG across all bands (Supplementary Fig. 3.3). Mosses on AP soil crusts exhibit such a spectral response (see fig. 3 in ref. 56). In addition, mosses of varied colour still exhibit NDVI values exceeding the threshold but have spectral signatures like those where the TCG threshold is not met (see figs. 5 and 6 in ref. 55). This supports the use of NDVI as the principal index and the resultant trends as presented in the main paper.

Cloud- and snow-cover masking

To remove cloud and snow cover from the imagery, the Fmask algorithm[57] was used. This step ensured that any vegetation signal measured was returned from clearly visible land. Consequently, for images to be comparable, similar amounts of ice-free land needed to be captured across images. Individual selection of persistently cloud- and snow-free pixels, or areas of pixels, across multiple images would be inefficient and generate too small of a sample area to be representative of AP scale changes. Hence obscured land percentage was derived from the area masked out by the Fmask algorithm (Supplementary Section 6). This indicated the amount of ice-free land observable for a given image.

Sampling strategy

To minimize known errors in earlier imagery, a buffered sample area strategy was utilized (Supplementary Fig. 2.1). First, the study area was divided into 5,000 km² hexagonal sample areas that covered all ice-free land areas. A hexagonal tessellation was used to systematically sample the region and for clear and comparable presentation of the data, as ice-free land areas in the region are orders of magnitude smaller than glaciated terrain and marine areas. For each hexagon and the overall study area, the Mann–Kendall test was conducted using the space–time analysis functions in ArcMap 10.8.1. Points representing the annual area of NDVI > 0.2 were generated at the centroid of each hexagon for each year. These points were then input into the Create Space Time Cube by Aggregating Points tool. Trend analysis was conducted on the maximum annual area, with no-data years treated as zeroes, using a 1 year time interval and a distance interval matching the hexagon height (76 km). Finally, the Visualize Space Time Cube in 2D tool was used to create the trend maps shown here. Ice-free land area was computed from previously published estimates of Antarctic ice-free topography[49]. A 300 m buffer around this map was generated to account for (1) high RMSE (root mean squared error) error in positioning from the use of Tier 2 imagery, (2) scan line corrector-off error in Landsat 7 imagery and (3) areas on land that are missing from previous estimates of ice-free topography on the AP[49] due to the masking of

snow and clouds over land (detailed in Supplementary Section 2.1 and Supplementary Fig. 2.1). Use of this buffer assumed that ice and snow were fully masked out by the cloud mask. In addition, it was assumed that negligible areas of NDVI values > 0.2 or positive TCG values were measured off land on unmasked ice and snow or at sea.

In early analysis, very small areas crossed thresholds for greening in both vegetation indices in the far south of the AP (for example, Alexander Island) and at higher latitudes elsewhere, far beyond the realistic latitudinal and altitudinal growing limit of moss-dominated ecosystems, even after recent rapid warming[29]. At high latitude and high altitude, illumination differences can cause bidirectional reflectance distribution function effects that result in erroneous returns in spectral indices[58]. To counter this, pixels with elevation values over 300 m on the reference elevation model of Antarctica[59] were masked out. A study on Signy Island (South Orkney Islands) identified a localized elevation threshold for moss banks at 120 m a.s.l.[60], but previous field-based research[22,23] observed similar moss systems at a maximum altitude of 220 m a.s.l., and so an altitudinal limit of 300 m a.s.l. was set at for this analysis, which eliminates the possibility of erroneous reflectance returns from high-relief topography in the south of the study region and allows a more reasonable window of detection for moss banks expanding to higher altitudes than currently observed (detailed in Supplementary Section 2.2 and Supplementary Fig. 2.2). Consequently, the measured signal represents the vegetated area with almost certain probability on unobscured areas of land below 300 m a.s.l.

Data availability
The Landsat 4, 5, 7 and 8 imagery is accessible via the code published along with this paper and from the Google Earth Engine data catalogue. The Hexbins employed in this study's analysis can also be reproduced using this code.

Code availability
The JavaScript code for extracting the annual maximum extent of pixels with NDVI > 0.2, TCG > 0 and total area of unmasked pixels in Google Earth Engine is archived at https://github.com/OllyBartlett/Roland_And_Bartlett_et_al_2024.

References
50. Gray, A. et al. Remote sensing reveals Antarctic green snow algae as important terrestrial carbon sink. *Nat. Commun.* **11**, 2527 (2020).
51. *Landsat Collection 1 Level 1 Landsat* (USGS, 2019).
52. Anderson, K. et al. Vegetation expansion in the subnival Hindu Kush Himalaya. *Glob. Change Biol.* **26**, 1608–1625 (2020).
53. Crist, E. P. & Cicone, R. C. A physically-based transformation of Thematic Mapper data—the TM Tasseled Cap. *IEEE Trans. Geosci. Remote Sens.* **22**, 256–263 (1984).
54. Crichton, K. A., Anderson, K., Bennie, J. J. & Milton, E. J. Characterizing peatland carbon balance estimates using freely available Landsat ETM+ data. *Ecohydrology* **8**, 493–503 (2015).
55. Puhovkin, A., Smykla, J., Váczi, P. & Parnikoza, I. Spectral characteristics of bryophyte carpet and mat subformation showing a vitality-dependent color pattern: comparison for two distant regions of maritime Antarctica. *Czech Polar Rep.* **13**, 96–111 (2023).
56. Fonseca, E. L., Dos Santos, E. C., De Figueiredo, A. R. & Simões, J. C. Antarctic biological soil crusts surface reflectance patterns from Landsat and Sentinel-2 images. *An. Acad. Bras. Cienc.* **94**, e20210596 (2022).
57. Zhu, Z., Wang, S. & Woodcock, C. E. Improvement and expansion of the Fmask algorithm: cloud, cloud shadow, and snow detection for Landsats 4-7, 8, and Sentinel 2 images. *Remote Sens. Environ.* **159**, 269–277 (2015).
58. Nagol, J. R. et al. Bidirectional effects in Landsat reflectance estimates: is there a problem to solve? *ISPRS J. Photogramm. Remote Sens.* **103**, 129–135 (2015).
59. Howat, I. M., Porter, C., Smith, B. E., Noh, M. J. & Morin, P. The reference elevation model of Antarctica. *Cryosphere* **13**, 665–674 (2019).
60. Cannone, N., Fratte, M. D., Convey, P., Worland, M. R. & Guglielmin, M. Ecology of moss banks on Signy Island (maritime Antarctic). *Bot. J. Linn. Soc.* **184**, 518–533 (2017).

Author contributions
T.P.R., O.T.B., D.J.C., K.A., I.M, D.A.H., P.T.F. and A.F. conceived the original idea for the work, following previous research and fieldwork undertaken by D.J.C, M.J.A., D.A.H. and T.P.R. The experimental design was collaboratively defined by O.T.B., T.P.R, D.J.C. and K.A. with O.T.B. and T.P.R. leading the practical implementation of the work. T.P.R. and O.T.B. led the writing of the paper with all authors contributing to and editing the text.

Competing interests
The authors declare no competing interests.

Additional information
Supplementary information The online version contains supplementary material available at https://doi.org/10.1038/s41561-024-01564-5.

Correspondence and requests for materials should be addressed to Thomas P. Roland or Oliver T. Bartlett.

Peer review information *Nature Geoscience* thanks Aleks Terauds and the other, anonymous, reviewer(s) for their contribution to the peer review of this work. Primary Handling Editor: Xujia Jiang, in collaboration with the *Nature Geoscience* team.

Reprints and permissions information is available at www.nature.com/reprints.